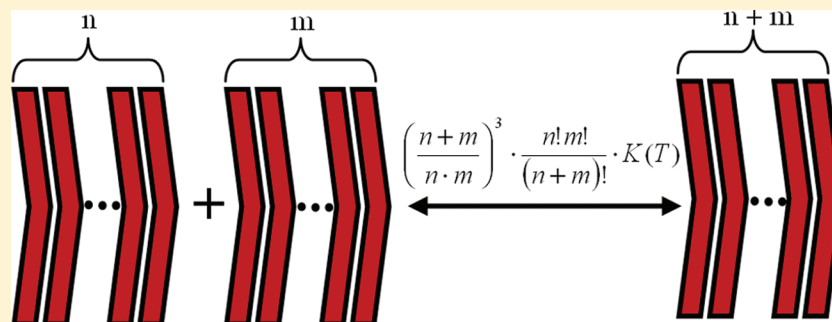


# Size Dependence of Molecular Self-Assembling in Stacked Aggregates. 1. NMR Investigation of Ciprofloxacin Self-Association

Ioan Turcu\* and Mircea Bogdan\*

Department of Molecular and Biomolecular Physics, National Institute of Isotopic and Molecular Technology, 400293 Cluj-Napoca, Romania



**ABSTRACT:** One of the most important purposes in molecular technologies is the preparation of supramolecular structures by self-assembling processes. The aromatic molecules self-associate mainly in  $\pi$ – $\pi$  stacked structures with an aggregate size distribution determined by the association equilibrium constants. A general expression for the equilibrium constants  $K_{n,m}$  which govern the self-association of two aggregates with  $n$  and  $m$  monomers respectively has been obtained. The model predicts also the concentrations of free monomers, the concentrations of  $n$ -mers, and the total concentration of aggregates.  $^1\text{H}$  NMR experiments have been used to illustrate the applicability of the proposed model in a particular case:  $\pi$ -stacking self-association of ciprofloxacin in solution.

## INTRODUCTION

Self-assembly is a ubiquitous natural process due to which individual entities organize themselves spontaneously into well-defined structures without any external instruction. In the case of molecular self-assembling, the specific association of molecules is performed through noncovalent interactions, including hydrogen and ionic bonds, and hydrophobic and van der Waals interactions.<sup>1–4</sup> The molecular self-assembly relies on non-covalent interactions, the key elements being the chemical complementarity and structural compatibility. Even if the individual interactions are weak, due to their large numbers, they will dominate the conformation of the built supramolecular structures. The materials built by self-assembly allow for a higher structural tunability, their bulk properties being imposed by the specific characteristics of individual monomeric building blocks. This feature leads to a new route to obtain novel materials with tailored morphologies and functions prepared through bottom-up single-molecule engineering.<sup>5,6</sup> A self-association process in solution seems to be extremely often encountered in the case of organic molecules that have aromatic rings.<sup>7–11</sup> The tendency is to aggregate into stacking structures which reduce the potential energy related to  $\pi$ – $\pi$  interaction and also the hydrophobic energy which depends mainly on solvent accessible surface area.<sup>12,13</sup>

The equilibrium size distribution of  $n$ -mers given by the equilibrium concentrations  $X_n$  depends on the association constants  $K_n$  which govern the stepwise self-association

processes where a monomer is captured by an aggregate with  $n - 1$  monomeric units. Among the huge numbers of papers dealing with such processes, different research teams use a variety of models which they consider appropriate for their particular field of interest.<sup>14–19</sup> The majority of them are based on an empirical relation between  $K_n$  and  $n$ , and by far the most used, is the EK-model<sup>18</sup> (isodesmic model) which assigns that all equilibrium self-association constants are equal. However, based on statistical thermodynamic grounds it has been shown that the isodesmic hypothesis is unreasonable<sup>20</sup> due to the entropy changes accompanying each self-association step. Another strong argument comes from experiments and is directly related to the fact that using the EK-model one obtains a systematic variation of the measured  $K$  values if the concentration range is changed. A relevant example is the NMR investigation of self-association of flavin mononucleotide, for which by changing the concentration ranges one obtains considerably different association constants.<sup>19,21</sup>

Self-association is one of the processes most directly related to the thermodynamic nonideality of the solute molecules. We consider that it is highly relevant to separate the intermolecular interactions in two distinct contributions:<sup>20</sup> the “associating” part which collects the main contribution to the nonideality and the

**Received:** February 6, 2012

**Revised:** May 10, 2012

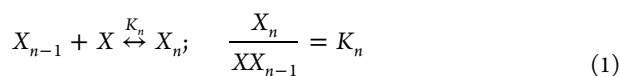
residual “nonassociating” contribution given mainly by the excluded volume effects and weak van der Waals forces. If a molecular system with an important self-association tendency is described as a single component solution, the virial expansion represents a quite bad approximation. The coefficients, which express quantitatively the nonideality are relatively large; they do not decrease (or decrease too slowly) with the expansion order and combine in an intricate manner the two contributions.<sup>20</sup> Alternatively, if the aggregates are treated explicitly the solution is expressed in a much more appropriate way as a multicomponent system. The most important part of the nonideality is included in the self-association constants, and the small nonassociating contribution can be described in terms of a residual virial expansion.

Several attempts have been made to overcome the simplicity of the EK-model and to describe in a more appropriate way the experimental results. On one side are the alternative models developed also empirically to provide simple analytical expressions suitable for further analysis of experimental data.<sup>17,18</sup> An alternative approach was dedicated to develop rigorous models based on physical grounds, and related directly to the well-known size dependent entropic contributions.<sup>14–16,19,22</sup> Unfortunately different papers, describing slightly different molecular systems, give different results for the fundamental question of size dependence of the self-association constants.

The main aim of our work is to develop an alternative rigorous theoretical approach based on statistical mechanics able to describe the self-association (dissociation) process of flat, pie-shaped monomers into one-dimensional aggregates. The solution is modeled as a nonideal system of aggregates which inter-relate each other by weak nonassociating interactions. A general expression for the equilibrium constants  $K_{n,m}$  which govern the self-association of two aggregates with  $n$  and  $m$  monomers respectively has been obtained. For a solution with a total concentration of monomers  $X_t$  ( $X_t = \sum_{n=1}^{\infty} nX_n$ ) the model predicts the concentrations of free monomers  $X$ , the concentrations of  $n$ -mers  $X_n$ , and also the total concentration of aggregates  $X_a$  ( $X_a = \sum_{n=1}^{\infty} X_n$ ) where the free monomer is also included as the first order aggregate  $X_1 \equiv X$ . All of these are the main ingredients used to predict the variation of the NMR measured chemical shift  $\delta_{\text{obs}}$  as a function of  $X_t$  and to assess the applicability of the proposed model in a particular case:  $\pi$ -stacking self-association of ciprofloxacin in solution.

## ■ SELF-ASSOCIATION MODELS

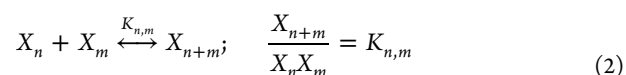
There are two main models that are usually applied in order to describe the molecular stepwise self-association processes.



One of them is the isodesmic model characterized by an equal association constant (EK model) at any step  $K_n = K$ . The other one is the attenuated  $K$  model (AK model) for which the equilibrium constant decrease with the length of the aggregate  $K_n = K/n$ . There are versions for both models that describe possible cooperative effects. Even if the above-mentioned models are often used and return apparently valuable results, they have not a solid physicochemical ground behind. Nevertheless they are frequently used because they are simple enough to get a compact analytic formula and also an easy fitting procedure for the experimental data.

In the following section a systematic assessment of the size effects on molecular self-assembling will be performed. All of the essential ingredients have statistical physics grounds and no empiric hypothesis will be introduced. As the model predicts a specific decrease of the binding efficacy with the increase of the aggregates size we will call it the decreasing  $K$  model (DK model) just to mark the difference from the above-mentioned AK model.

**Decreasing  $K$  Model.** A self-association (dissociation) process in which a one-dimensional aggregate with  $n+m$  monomers is created from (or dissociate into) two aggregates with  $n$  and  $m$  monomers is described by the following scheme:



At equilibrium, under normal laboratory conditions of constant temperature and pressure, the chemical potentials of the involved aggregates are related by

$$\mu_n + \mu_m = \mu_{n+m} \quad (3)$$

The chemical potential for aggregates can be given conveniently in the following form:

$$\mu_n = \mu_n^{\text{ig}} + \Delta G_n^{*\text{sol}}; \quad \mu_n^{\text{ig}} = -kT \ln \left( \frac{q_n}{\Lambda_n^3 X_n} \right) \quad (4)$$

where  $\mu_n^{\text{ig}}$  is the chemical potential in the ideal gas state,  $q_n$  the aggregate internal partition function,  $\Lambda_n = h/(2\pi m_n kT)^{1/2}$  the de Broglie wavelength,  $h$  the Planck constant,  $m$  the mass of the monomer ( $m_n = n \cdot m$ ), and  $\Delta G_n^{*\text{sol}}$  the Ben Naim solvation free energy<sup>23</sup> of the  $n$ -mer. The free energy of solvation  $\Delta G_n^{*\text{sol}}$  is the work needed to transfer an aggregate from a fixed position in an ideal gas to a fixed position in solution at constant temperature and pressure. We must stress here that the simplicity and compactness of eq 4 is only a formal one, and all the difficulties related to the accurate description of a relatively complex molecular system are in fact included in  $\Delta G_n^{*\text{sol}}$ . Just to maintain the model at a reasonable degree of complexity we will describe the solvation free energy in a phenomenological way, using the simplest approximations.

Using eqs 3 and 4 the association constant  $K_{n,m}$  can be obtained if the information about the inner molecular properties on one side and about the solvent-aggregate interaction on the other side is available

$$kT \ln K_{n,m} = kT \ln \left( \frac{q_{n+m}}{q_n q_m} \cdot \frac{\Lambda_n^3 \Lambda_m^3}{\Lambda_{n+m}^3} \right) + \Delta G_{n+m}^{*\text{sol}} - \Delta G_n^{*\text{sol}} - \Delta G_m^{*\text{sol}} \quad (5)$$

If we accept for the aggregates the rod-like linear model one can neglect in the first approximation the aggregate vibrations and describe the aggregate internal partition function  $q_n$  taking into consideration only the monomer internal partition function  $q_{\text{int}}$ , the rotational degrees of freedom and the cumulative energetic contribution  $W_n$  of two main interactions: the localized intermonomeric short-range forces and the global electric potential, respectively

$$q_n \approx \frac{q_{\text{int}}^n e^{-W_n/kT} \cdot q_n^{\text{rot}}}{n!} = \frac{q_{\text{int}}^n e^{-W_n/kT}}{n!} \frac{\sqrt{\pi}}{\sigma} \left( \frac{8\pi^2 kT}{h^2} \right)^{3/2} \left( \prod_{i=1}^3 I_n^{(i)} \right)^{1/2} \quad (6)$$

In eq 6  $I_n^{(i)}$  are the three moments of inertia of the aggregate and the symmetry factor  $\sigma$  stands for the number of ways in which the aggregate can reach by rotation the same spatial orientation. If the aggregates are approximated with cylinders,  $I_n^{(i)}$  are given by

$$I_n^{(1)} = n \frac{mR^2}{2}; \quad I_n^{(2)} = I_n^{(3)} = n(3 + n^2\varepsilon) \frac{mR^2}{12} \quad (7)$$

The parameter  $\varepsilon = (L/R)^2$  quantify the square ratio of the monomer effective thickness  $L$  to the monomer mean radius  $R$  and is a small number for flat, pie-shaped monomers. In the case of weak binding the majority of aggregates incorporate a relatively small number of monomers and consequently the contribution of the term which depends on the small parameter  $\varepsilon$  will be neglected.

To going further one must emphasize two distinct cases that must be carefully analyzed.

**a. Uncharged Monomers.** If the monomeric units are uncharged it is usually accepted that the electronic contribution to the stability of the aggregate is brought only by a nearest neighbor interaction.<sup>24,25</sup> Accordingly, if each interface between two monomers bring the energy  $w$ , the total energy corresponding to a  $n$ -mer is  $W_n = (n - 1)w$ .

**b. Charged Monomers.** In the case of charged monomers, each aggregate is accompanied by a diffuse cloud of counterions and an additional electrostatic potential energy must be taken into account:  $W_n = (n - 1)w + nw_{el}$ . The additional contribution is proportional to the size of the aggregate,<sup>26</sup>  $w_{el}$  standing for the electrostatic potential energy per monomer. Of course, the screened electric field diminishes to some extent the intermonomeric attraction and therefore decreases also the interfacial contribution  $w$ . For our purposes it is not important to present analytic expressions for these parameters and we will take both  $w$  and  $w_{el}$  as phenomenological parameters. However, it is important to stress the essential difference between them: although  $w$  is given mainly by the  $\pi$ - $\pi$  interaction between neighboring molecular orbitals and depends on local electronic charge distribution,  $w_{el}$  is given in terms of ionic charge distribution and depends on the total concentration of the monomers that dissociate in the solvated state. Nevertheless, due to its linear dependence on the aggregate size the electrostatic energy of an aggregate with  $n + m$  monomers is equal to that of the two aggregates with  $n$  and  $m$  monomers respectively and hence, the aggregation (dissociation) processes do not change the electrostatic energy. As a direct consequence,  $w_{el}$  and its dependence on the total concentration of monomers do not affect the association constants.

As concerning the solvation free energy, we will use the frequently accepted surface tension approximation

$$\Delta G_n^{*sol} \approx \gamma A_n = \gamma(A_l + A_r + nA_s) \quad (8)$$

where  $A_l$ ,  $A_r$ , and  $A_s$  stand for the effective left side, right side and lateral areas of the monomeric unit. The surface tension  $\gamma$  will be taken also as a phenomenological parameter, and together with  $w_{el}$  is an additional source of nonideality being weakly dependent on the total concentration of monomers. Without going into details, the main cause of this dependence is the excluded volume effects. Accordingly, one can neglect in first approximation the particular way in which the total volume of the monomers is distributed among different aggregates and keep only the main feature, namely the relatively weak dependence on the total concentration of monomers:  $\gamma \approx \gamma_0 + \gamma_1 X_t$ .

From eqs 5–8, one gets the dependence of the association constants  $K_{n,m}$  on the length of the associated aggregates

$$K_{n,m}(T) = \left( \frac{n+m}{nm} \right)^3 \frac{n!m!}{(n+m)!} K(T);$$

$$K(T) \approx K_0(T) e^{\Gamma(T)X_t} \quad (9)$$

$K_0(T)$  collects the terms that do not depend on the length of the aggregates and on solvate concentration, its specific expression is irrelevant to the reasoning that follows and therefore it can be thought as a phenomenological parameter. On the other side it is important to stress here that keeping the model as simple as possible one can incorporate as well, in a rough approximation, the weak nonassociative nonideality coming mainly from the solvation free energy. This contribution is described in the simplest way by  $\Gamma(T) = \gamma_1(A_l + A_r)/kT$ . Invoking arguments that are similar to that used for the electrostatic energy, the terms proportional to the number of monomers in eq 8 compensate in an associative process and do not affect the association constant. This compensating behavior is a general property of nonideal systems of molecular aggregates for which the activity coefficient is proportional to the aggregate size.<sup>27</sup> Even if  $K_0$  and  $\Gamma$  have the same units ( $M^{-1}$ ) only  $K_0$  is a true association constant.  $\Gamma$  is just the additional parameter designated to describe the nonassociative component of the system nonideal behavior. The applicability of the model is limited to total concentrations that are small enough to ensure the inequality  $\Gamma X_t < 1$ . This inequality expresses in a quantitative way the smallness of the nonassociative interactions.

It is obvious that the crude approximations invoked above are not able to describe the multiple aspects related to the nonideality of the molecular self-association processes<sup>28</sup> but we consider that the proposed model can be a reasonable compromise being simple enough for a relatively large accessibility while incorporating the basic phenomenology.

It is important to note that the size dependence in eq 9 originate from three different contributions. The translational and rotational partition functions of the aggregates bring, each of them, a contribution proportional to  $((n+m)/nm)^{3/2}$ . The term  $n!m!/(n+m)!$  comes from the combinatorial factors that take into account the identity of monomers in the aggregates. The model that we describe combines the one particle properties of the aggregates (one body translational and rotational motions) with the statistical attributes (combinatorial factors) of composite systems made from indistinguishable monomers. The main argument for introducing indistinguishability is the very fast exchange between free monomers and those stacked in aggregates attested by the NMR spectra for example. If the monomers from a stack would be fixed then one would expect to find different chemical shifts for the bound and free monomers respectively. Instead to find such an NMR response the measured spectra shown a single peak which collect the weighted contribution of both free and bound monomers. A completely different behavior is encountered in the case of molecular crystals for example. In the statistical description of such systems, even if the molecules are identical from the chemical point of view, they can be recognized as different objects due to their well-defined spatial position.

In order to obtain the concentration of each  $n$ th order aggregate ( $n$ -mers), we come back to the stepwise self-association processes and find the expressions for corresponding association constants

$$K_n \equiv K_{n-1,1} = \frac{K}{n} \left( \frac{n}{n-1} \right)^3 \quad (10)$$

In eq 10 (and in the following also) the  $T$  dependence of  $K(T)$  has been omitted for simplicity reasons.

Starting from the general relation described in eq 9 one predict the size dependent equilibrium constant of the stepwise self-association processes, given by eq 10, as a particular case. It is important to stress that the predictions are similar with that obtained in ref 19 which confirms the suitability of the used hypothesis.

In Figure 1 the size dependence of the self-association constants are given for several association models. Besides the

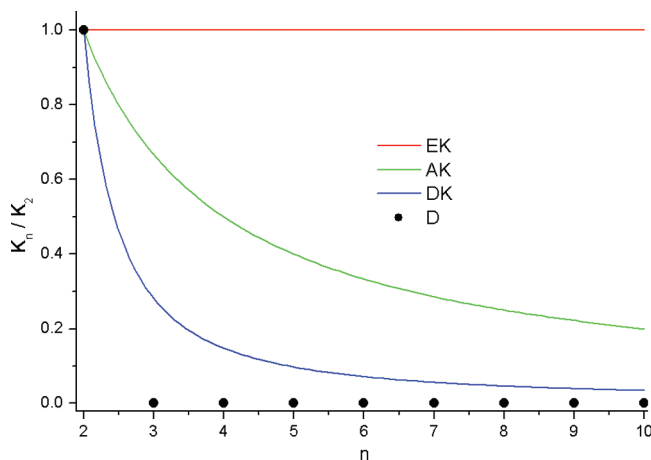


**Figure 1.** Size dependence of the stepwise self-association for several association models: EK, AK, DK, and D.

EK, AK, and DK models we have shown also the typical behavior of the simplest process: the dimerization (D-model) for which the only nonzero equilibrium constants is  $K_2$ . From a formal point of view the AK and DK models describe association processes having an intermediate behavior between the size independent EK-model and the step-type dependence shown by D-model. It is important to realize that it is a one to one relation between  $K_2$  and  $K$ , relation which is model dependent:  $K_2 = K$  for D and EK models;  $K_2 = K/2$  for AK model; and  $K_2 = 4K$  for DK model respectively. Comparing the DK and AK models one can see that for DK,  $K_n$  shown a more pronounced decrease, approaching (in this formal sense) the dimerization D-model. This means that it is one of the most unfavorable for the appearance of big aggregates among the other frequently used models. Such a behavior can be found explicitly in eq 9 which return the smallest self-association efficiency (the highest breaking tendency) for  $n = m$ . In other words the aggregates are most likely to fragment in the middle (the annealing of two aggregates with a similar size is extremely improbable) and to grow by capturing an additional monomer at the ends.

**Size Distribution of Aggregates.** *a. Associative Contribution.* If the concentration dependence of the association constant is neglected, ( $K \approx K_0$ ), it is straightforward to prove using eqs 1 and 10 that the concentration of any  $n$ -mer can be expressed simply as an  $n$ -order power function of the monomer concentration

$$X_n = \frac{1}{n} \left( \frac{n}{n-1} \right)^3 X_{n-1} K_0 X = \prod_{p=2}^n \frac{1}{p K_0} \left( \frac{p}{p-1} \right)^3 (K_0 X)^n \quad (11)$$

or equivalently

$$x_n(x) = \frac{2^2 \cdot 3^2 \cdots (n-1)^2 \cdot n^2}{1^3 \cdot 2^3 \cdot 3^3 \cdots (n-1)^3} (K_0 X)^n = \frac{n^3}{n!} x^n \quad (12)$$

The notation  $x$  and  $x_n$ , and in the following  $x_v$ ,  $x_a$  stand for the adimensional concentrations  $x = K_0 X$ ,  $x_n = K_0 X_n$ ,  $x_t = K_0 X_t$ ,  $x_a = K_0 X_a$ . The sums

$$X_a = \sum_{n=1}^{\infty} X_n; \quad X_t = \sum_{n=1}^{\infty} n X_n \quad (13)$$

giving the concentration of aggregates and the total concentration of monomers, respectively, can be performed analytically and in form of  $x_a$  and  $x_t$  are expressed as

$$\begin{aligned} x_a(x) &= \sum_{n=1}^{\infty} x_n \\ &= \left( x \frac{d}{dx} \right)^3 \sum_{n=1}^{\infty} \frac{x^n}{n!} \\ &= \left( x \frac{d}{dx} \right)^3 (e^x - 1) \\ &= \Phi_3(x) \end{aligned} \quad (14)$$

where the functions  $\Phi_n(x)$  are defined by  $\Phi_n(x) = (x(d/dx))^n e^x$ . The expressions of the first five functions  $\Phi_n(x)$  are given below

$$\begin{aligned} \Phi_1(x) &= x e^x \\ \Phi_2(x) &= (x + 1) x e^x \\ \Phi_3(x) &= (x^2 + 3x + 1) x e^x \\ \Phi_4(x) &= (x^3 + 6x^2 + 7x + 1) x e^x \\ \Phi_5(x) &= (x^4 + 10x^3 + 25x^2 + 15x + 1) x e^x \end{aligned} \quad (15)$$

The concentration of free monomers  $x$  and the total concentration monomers  $x_t$  are related by the conservation of the total number of monomers

$$x_t(x) = \sum_{n=1}^{\infty} n x_n = \left( x \frac{d}{dx} \right) x_a = \Phi_4(x) \quad (16)$$

Equation 16 reveals also a general relation between  $x_v$ ,  $x_a$

$$\frac{dx_a}{dx} = \frac{x_t}{x} \Leftrightarrow x_a(x) = \int_0^x \frac{x_t(x)}{x} dx \quad (17)$$

which is independent of any particular model.<sup>29</sup> The mean number of monomers in an aggregate (considering the monomer as the aggregate with one particle) can be expressed also in a very simple manner by the ratio of the two concentrations at equilibrium

$$\langle n \rangle = \frac{\sum_{n=1}^{\infty} n x_n}{\sum_{n=1}^{\infty} x_n} = \frac{x_t}{x_a} = \frac{\Phi_4(x)}{\Phi_3(x)} \quad (18)$$

The importance of the mean number of monomers in an aggregate  $\langle n \rangle$  will become clearer in the following chapter where we will show that it is the only parameter that controls the



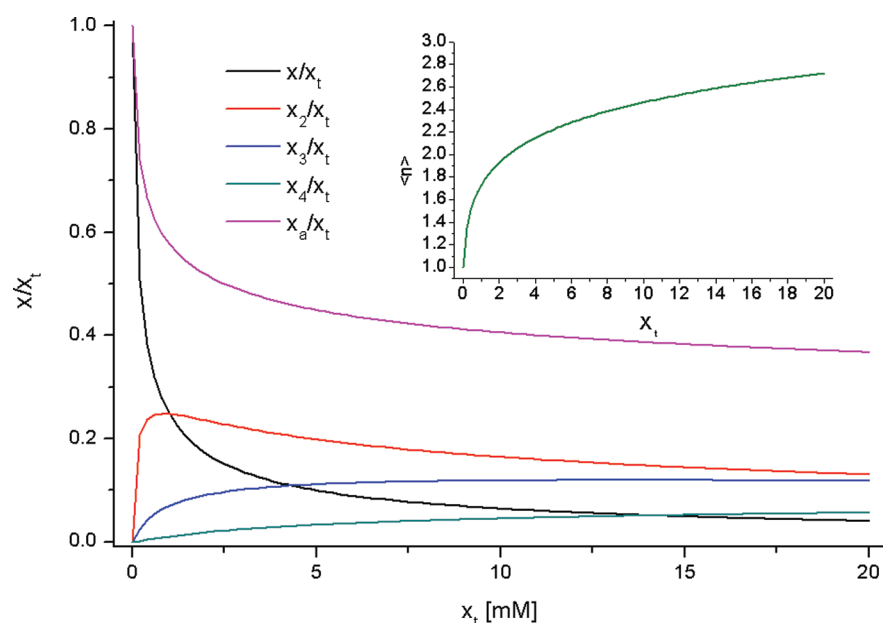


**Figure 2.** Variation of the relative abundance of several  $n$ -mers predicted by the DK model. Inset: the increase of aggregates mean size ( $K_0 = 10^3 \text{ M}^{-1}$ ).

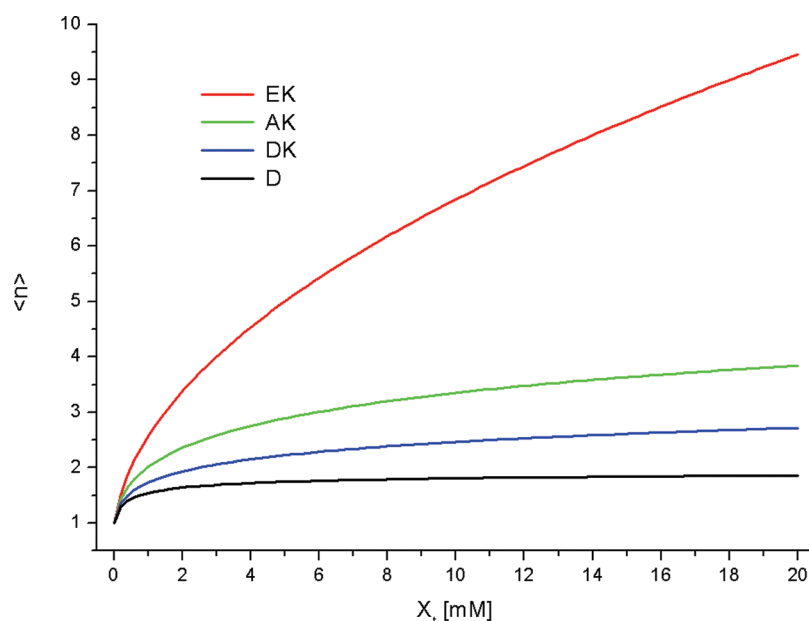


**Figure 3.** Comparison of the variation of the mean aggregate size with the total concentration of monomers predicted by four self-association models: EK, AK, DK, and D ( $K_2 = 4 \times 10^3 \text{ M}^{-1}$ , equivalently with  $K_0 = 10^3$  for the DK model).

displacement of the NMR chemical shift in the self-associating molecular systems.

The last step is to invert eq 16 in order to obtain  $x(x_t)$ . The main difficulty encountered now is that for the investigated model the equation is transcendental and the inversion cannot be performed analytically. Even if for simpler empirical models this task can be done (for third order or quartic equations for example), one obtains long and tedious formula which are not recommended for direct numerical evaluation.<sup>30</sup>

The alternative way is to follow the procedure developed by Poon<sup>30</sup> for the titration calorimetry experiments. The idea is to solve numerically a first-order ordinary differential equation (ODE) with total concentration  $x_t$  as independent variable and the concentration of free monomers  $x$  as dependent variable. The

ODE can be obtained straightforwardly by differentiation with respect to  $x_t$  the first and last term of eq 16

$$1 = \frac{dx}{dx_t} \frac{d\Phi_4(x)}{dx} \rightarrow \frac{dx}{dx_t} = \frac{x}{\Phi_5(x)}; \quad x(0) = 0 \quad (19)$$

The dependence  $x(x_t)$  for a fixed  $K$  being obtained by numerical integration, eqs 12 and 14 give explicitly the  $x_t$  dependence of the concentration of each  $n$ -mer and of the total concentration of aggregates.

Figure 2 shows a typical size distribution predicted by the DK model. One must remark the sharp increase of dimers relative abundance at low concentrations of monomers, followed by slow decrease of their relative abundance at higher concentrations. As expected, the relative population of monomers (and of

aggregates also) decrease continuously with the increase of the number of  $n$ -mers with growing  $n$ .

As the mean number of monomers in an aggregate  $\langle n \rangle$  is a highly relevant parameter in a self-association process we show in Figure 3 the increase of this number with the increase of the total concentration of monomers for the four models nominated above.

One can see that the dependence predicted by the dimerization (D) model is limited to 2 (being therefore unnaturally small for an indefinite self-association process) and increase with a relatively high rate in the case of EK model. The AK and DK models predict more realistic increases, correlated with the size dependence of their self-association constants shown in Figure 1.

**b. Nonassociative Contribution.** The ideal case can be extended in a relatively simple way to the nonideal systems by modifying slightly the eq 11

$$\begin{aligned} X_n &= \frac{1}{n} \left( \frac{n}{n-1} \right)^3 X_{n-1} K_0 e^{\Gamma X_t} \\ &= \prod_{p=2}^n \frac{1}{p(K_0 e^{\Gamma X_t})} \left( \frac{p}{p-1} \right)^3 (K_0 e^{\Gamma X_t})^n \end{aligned} \quad (20)$$

It is easy to observe that eq 20 becomes similar to eq 11 if  $X_n$  is replaced by  $Y_n \equiv X_n e^{\Gamma X_t}$ . The similarity goes further and one can write

$$\begin{aligned} y_n &\equiv x_n e^{\alpha x_t} = \frac{n^3}{n!} y^n; \quad y \equiv x e^{\alpha x_t}; \quad \alpha = \frac{\Gamma}{K_0} \\ x_a(y, x_t) &= e^{-\alpha x_t} \Phi_3(y); \quad x_t(y, x_t) = e^{-\alpha x_t} \Phi_4(y); \quad \langle n \rangle \\ &= \frac{\Phi_4(y)}{\Phi_3(y)} \end{aligned} \quad (21)$$

The ODE in the nonideal case is obtained also in a relatively straightforward way

$$\begin{aligned} (1 + \alpha x_t) e^{\alpha x_t} &= \frac{d\Phi_4(y)}{dy} \frac{dy}{dx_t} \rightarrow \frac{dy}{dx_t} \\ &= \frac{(1 + \alpha x_t) e^{\alpha x_t} y}{\Phi_5(y)}; \quad y(0) = 0 \end{aligned} \quad (22)$$

It is easy to verify that it eq 22 goes to eq 19 in the limit  $\alpha \rightarrow 0$ . The dependence  $y(x_t)$  can be obtained now by numerical integration of eq 22. For relatively small values of  $\alpha$  ( $\Gamma X_t < 0.1$  in the entire domain of concentrations for example) the relative abundance depicted in Figures 2 and 3 keeps similar shapes, small deviations appearing in the range of higher values of  $X_t$ .

It is important to stress here that the developed model is independent of any type of experimental technique. The predictions of the model can be checked by using different spectroscopic or calorimetric methods, analytical centrifugation or any other techniques that are sensitive to self-association phenomena. Data sets obtained by a certain experiment can be fitted by the DK model to find the unknown specific parameters. In the following we will assess the suitability of the model to describe the self-association process from  $^1\text{H}$  NMR data.

## NMR ASSESSMENT OF SELF-ASSOCIATION PROCESSES

The  $^1\text{H}$  NMR signals of different protons of the monomer are affected in a different manner by the self-association process,

depending on the strength of their interaction with other monomers in the stack. The generally accepted hypothesis is that for a linear self-assembling process the influence is mainly limited to the first neighbors. If the monomer architecture has an intrinsic asymmetry then the chemical shift of the external monomers can be also asymmetrically affected by the left or right neighbor respectively

$$\Delta\delta_l = \delta_f - \delta_l; \quad \Delta\delta_r = \delta_f - \delta_r \quad (23)$$

In eq 23  $\delta_f$  stands for the chemical shift of the free monomer, and  $\delta_l, \delta_r$  for the displaced chemical shifts of the monomers placed on the left/right side respectively. This influence is experienced by the first and last molecule from each aggregate.

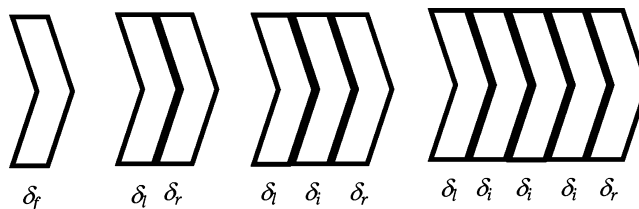


**Figure 4.** Contribution to the chemical shift brought by the inner/external monomers in aggregates with increasing length.

Any other inner monomer cumulates the effect coming from both left and right neighbors  $\Delta\delta = \Delta\delta_l + \Delta\delta_r$  and its chemical shift  $\delta_i$  becomes

$$\delta_i = \delta_f - \Delta\delta \quad (24)$$

Consequently the mean chemical shift per monomer in an  $n$ -mer is obtained by the weighted average contribution coming from the external and internal monomers respectively

$$\begin{aligned} \delta_n &= \frac{\delta_l + \delta_r + (n-2)\delta_i}{n} = \delta_f - \frac{(n-1)\Delta\delta}{n} \\ \delta_l &= \delta_f; \quad \delta_n \xrightarrow{n \rightarrow \infty} \delta_i \end{aligned} \quad (25)$$

Typically the self-association processes have a relatively fast dynamics, and one cannot obtain individual NMR peaks from different aggregates. The measured NMR signal is just the weighted average contribution coming from the aggregates of any order which populate the solution

$$\begin{aligned} \delta_{\text{obs}} &= \frac{1}{X_t} \sum_{n=1}^{\infty} n X_n \delta_n \\ &= \delta_f - \Delta\delta \left( 1 - \frac{X_a}{X_t} \right) \\ &= \delta_f - \Delta\delta \left( 1 - \frac{1}{\langle n \rangle} \right) \end{aligned} \quad (26)$$

It is important to stress that eq 26 has a general validity and is suitable for any self-association process. A particular model describing the process lead to a specific dependence of  $X_a$  on  $X_t$  and specify also the variation of  $\delta_{\text{obs}}$  with  $X_t$ . For very dilute solutions the contribution to  $X_a$  is brought almost only by the monomers ( $X_a \approx X_t$  or equivalently  $\langle n \rangle \approx 1$ ) and  $\delta_{\text{obs}}$  is close to the monomer value  $\delta_f$ . By increasing the total concentration of monomers  $X_t$ , due to the self-association process, the increases of  $X_a$  remain progressively behind  $X_t$  and consequently the measured chemical shift will deviate gradually from  $\delta_f$ .

Although rarely explicitly described, from any envisaged self-association model, there are two major bottlenecks that must be overcome: (i) to get analytic expressions for  $X_n(X)$ ,  $X_a(X)$ , and  $X_t(X)$  which depend all of them only on the monomer concentration  $X$  and (ii) to succeed in inverting the function  $X_t(X)$  and to get the variation of free monomer concentration with the total concentration of monomers  $X(X_t)$ . If these two tasks are overcome, from eq 26 one can find straightforwardly the dependence  $\delta_{\text{obs}}(X_t)$  and use this function to fit the measured  $^1\text{H}$  NMR data.

For fixed values of  $K_0$  and  $\Gamma$  eq 22 can be integrated numerically and the function  $y(x_t)$  can be used to obtain the  $X_t$  dependence of  $\delta_{\text{obs}}$  by replacing  $\langle n \rangle$  from eq 22 into eq 26

$$\delta_{\text{obs}}(X_t) = \delta_f - \Delta\delta \left\{ 1 - \frac{\Phi_3[y(K_0 X_t)]e^{-\Gamma X_t}}{K_0 X_t} \right\} \quad (27)$$

The essence of interpreting NMR data in a self-association process lies in modeling the behavior of  $\delta_{\text{obs}}(X_t)$ . The strategy we propose here is to formulate explicitly the ODE in terms of the independent variable  $x_p$ , a suitable dependent variable  $y(x_t)$  and two specific parameters:  $K_0$  and  $\Gamma$ . First, using the numerical integration of ODE we get the chemical shifts  $\delta_{\text{obs}}(X_t^{(p)}, K_0, \Gamma, \delta_f, \Delta\delta)$  computed for the same  $X_t^{(p)}$  ( $p = 1, 2, \dots, N$ ) values for which the experimental data  $\delta_{\text{obs}}^{(p)}$  have been measured. Like  $K_0$  and  $\Gamma$  the other two parameters  $\delta_f$  and  $\Delta\delta$  are fixed at reasonable values and all of them will be obtained in the next step by the fitting procedure. After that, the residual sum of squares is generated

$$S = \sum_{p=1}^N |\delta_{\text{obs}}^{(p)} - \delta_{\text{obs}}(X_t^{(p)}, K_0, \Gamma, \delta_f, \Delta\delta)|^2 \quad (28)$$

and the parameters  $K_0$ ,  $\Gamma$ ,  $\delta_f$  and  $\Delta\delta$  are optimized in order to minimize the residual sum of squares. Since most of the nonlinear least-squares algorithms involve evaluation of partial derivatives of  $S$  with respect to the parameters, data fitting is best accomplished by coupling the ODE solver to an optimization routine that incorporates numerical differentiation, rather than one that requires analytical derivatives from the user.

For fitting the experimental data we used Origin data analysis software which can be interfaced with external NAG library to perform numerical ODEs within its nonlinear regression routines. Using Origin's (OriginLab) code builder, an appropriate fitting program was developed which combines, at each iteration step, the parameters optimizing routine with the numerical integration procedure of the ODE defined in eq 22.

## NMR ASSESSMENT OF CIPROFLOXACIN SELF-ASSEMBLING

Extensive use of aromatic compounds in clinical practice and in different biophysical studies at the molecular and cellular levels is due to their great biological and medical activity. In addition, it has been shown that the biological activity of aromatic compounds may be substantially changed when inclusion complexes between these drugs and cyclodextrins (CDs) are formed in order to increase their bioavailability.<sup>31,32</sup> In an attempt to characterize the complexation process between ciprofloxacin, a synthetic chemotherapeutic antibiotic of the fluoroquinolone drug class and  $\beta$ -CD by NMR titration experiments, we observed that the inner  $\beta$ -CD protons exhibit very small chemical shift changes, whereas for ciprofloxacin protons the observed induced chemical shifts variation were at least an order of magnitude higher. A plausible explanation for

this finding is that ciprofloxacin molecules have a relatively low affinity to  $\beta$ -CD but they have a significant tendency to self-associate in aqueous solution. A similar process of self-association was put in evidence for ciprofloxacin encapsulated in liposomes.<sup>33</sup> It has been shown<sup>18</sup> that at mM concentrations in aqueous solution, there is a strong tendency for aromatic drugs to exhibit self-association, forming dimers and higher order aggregates which are stabilized by  $\pi$ - $\pi$  stacking interactions. Depending on the experimental method applied, different models have been used to analyze self-association of aromatic compounds. Dimer models are mostly used to interpret spectrophotometric data,<sup>34</sup> taking into account the formation aggregates with no more than two molecules in the stack. The dimer model is appropriate only when the concentration and the equilibrium association constants of the interacting molecules are small.<sup>35,36</sup> When comparatively large concentrations of molecules are used in the experiment, such as for NMR investigation for example, more general models which take into account the indefinite self-association of aromatic molecules in solution must be used. The assumptions used in NMR modeling of the association of aromatic molecules in solution are discussed in a review on the comparison of indefinite self-association models.<sup>33</sup> NMR spectroscopy has some advantages over optical investigations of molecular self-association in solution because it can be used to determine both the equilibrium and structural details of aggregates formation in solution.<sup>37</sup>

In the present work the experimental data obtained by measuring the displacement of chemical shifts of ciprofloxacin protons have been processed in the framework of DK-model in order to assess its suitability.

## EXPERIMENTAL SECTION

**Materials.** Ciprofloxacin hydrochloride (Figure 5) was kindly provided by Pharmaceutical Faculty, Cluj-Napoca and was of

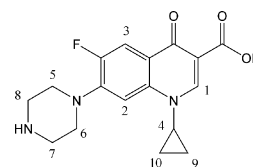


**Figure 5.** Chemical structure of ciprofloxacin. Numerals correspond to proton positions referred to in the NMR study.

pharmaceutical grade. Deuterium oxide (99.5% isotopic purity) was manufactured by Heavy Water Plant ROMAG PROD, Romania. The samples for NMR measurements were prepared by dissolving the ciprofloxacin in  $\text{D}_2\text{O}$  to obtain a stock solution of 70 mM. The stock solution was diluted with  $\text{D}_2\text{O}$  to obtain samples with concentrations in the range 0.25–70 mM for ciprofloxacin.

**Method.** All of the 1D and 2D NMR spectra were recorded on a Bruker Avance III 500 FT NMR spectrometer operating at 500.13 MHz for  $^1\text{H}$  and 470.53 MHz for  $^{19}\text{F}$ . All experiments were carried out in  $\text{D}_2\text{O}$  at a temperature of 298 K. The  $^1\text{H}$  and  $^{19}\text{F}$  NMR spectra were recorded using a simple pulse-acquire sequence. For  $^1\text{H}$  NMR spectra, typical acquisition parameters consisted of 32 K points covering a sweep width of 5000 Hz and a pulse width of 10  $\mu\text{s}$ . Depending on the sample concentrations, the number of scans ranged from 4 to 64 with a relaxation delay of 3 s. For  $^{19}\text{F}$  NMR spectrum, eight scans were measured into 64 K data points at a spectral width of 6579 Hz. The chemical shift

values are reported in ppm relative to TMS for  $^1\text{H}$  NMR spectra and  $\text{CFCl}_3$  for  $^{19}\text{F}$  NMR spectrum. Signal assignments of ciprofloxacin protons were made in accordance with  $^1\text{H}$  NMR spectra published previously for ciprofloxacin and related fluoroquinolones.<sup>38,39</sup> The H2 and H3 protons were distinguished by the relative splitting of the signal. Due to its close proximity to the fluorine in the ortho position, H3 was assigned to the signal with the larger coupling constant. In order to check this assumption a  $^{19}\text{F}$  expanded spectrum of ciprofloxacin is presented in Figure 6. As can be seen, the spectrum consists in a

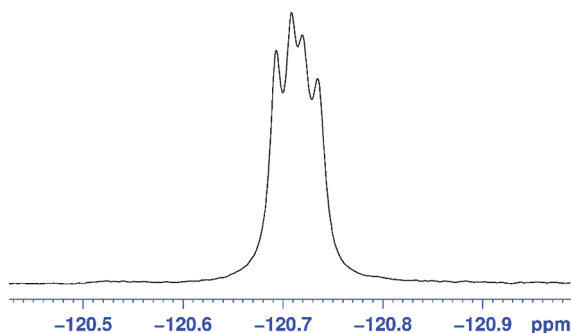


Figure 6. Expanded  $^{19}\text{F}$  spectrum of ciprofloxacin.

doublet of doublets with  $^3J_{\text{F-H}} = 12.6$  Hz and  $^4J_{\text{F-H}} = 7.2$  Hz. The same coupling constants were observed in the  $^1\text{H}$  NMR spectrum of ciprofloxacin (Figure 7).

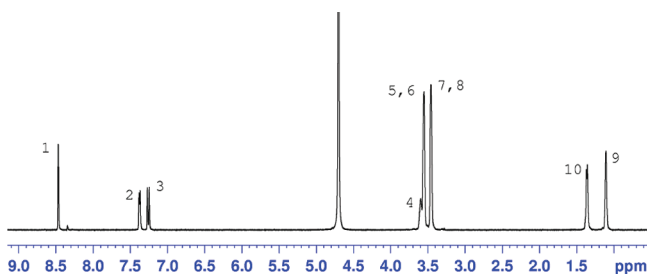


Figure 7.  $^1\text{H}$  NMR spectrum of ciprofloxacin in  $\text{D}_2\text{O}$  at 30 mM.

The  $^1\text{H}$  NMR ROESY spectrum of a 30 mM ciprofloxacin solution in  $\text{D}_2\text{O}$  is depicted in Figure 8. The ROESY spectrum was acquired on a 30 mM ciprofloxacin aqueous solution in the

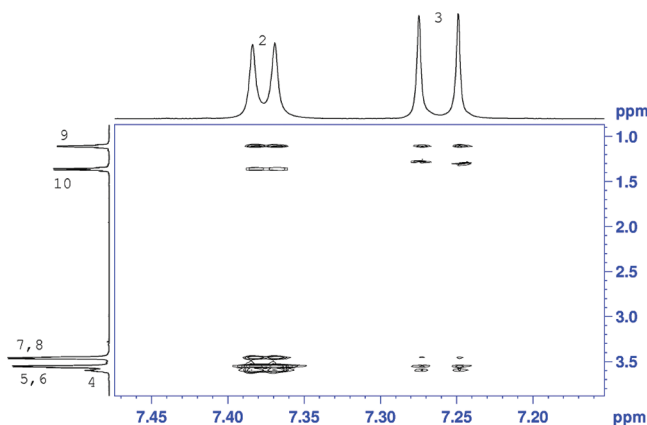


Figure 8. Expanded region of the 2D  $^1\text{H}$  NMR Spectrum of ciprofloxacin.

phase sensitive mode and residual water suppression, using Bruker standard parameters (pulse program roesyphpr).

The spectrum consisted of a matrix of 8 K (F2) by 4 K (F1) points covering a spectral width of 5000 Hz. The spectrum was obtained with a spin – lock mixing time of 250 ms, relaxation delay 3 and 4 scans were recorded.

A possible structure of the ciprofloxacin dimers in solution can be proposed based on the observed intermolecular cross peaks in the 2D ROESY spectrum.

As can be seen in Figure 8, there are intensive cross peaks between H2 and H3 protons with all other protons belonging to ciprofloxacin, except H1. This is clear evidence that ciprofloxacin molecules form stacks in aqueous solutions where, as a consequence of  $\pi$ – $\pi$  interactions, the molecules lie on top of each other in an antiparallel orientation. This specific orientation minimizes also to repulsive interaction between the local charge of each ciprofloxacin cation. It is worth noting that the crystal structure of some drugs belonging to quinolone family shows also intermolecular self-association, the molecules lying on top of each other in a head to tail arrangement.<sup>36</sup>

## RESULTS AND DISCUSSION

Alongside many aromatic molecules in aqueous solution, the appearance of stacked aggregates of ciprofloxacin is reflected also by the strong concentration dependence of proton chemical shifts of the drug molecules. The curves showing the dependence  $^1\text{H}$  NMR chemical shifts with ciprofloxacin concentration for four most sensitive protons are shown in Figure 9. For all protons which are significantly affected by self-association chemical shifts are displaced to lower values with the increasing concentration of the drug. The  $^1\text{H}$  NMR lines are not significantly widened at any concentration. In the case of ciprofloxacin self-association, chemical shifts of the aromatic protons H1, H2, and H3 from the 4-quinolone ring experience significantly larger changes with concentration compared with the H4 proton for example. The last several data corresponding to the high concentration range are missing in the curve giving the chemical shift of H4 due to the fact that the NMR lines of protons H4, H5, and H6 (see Figure 6) become indiscernible in the concentrations range higher than 50 mM. The effect of ciprofloxacin concentration on the shift of the other nonaromatic proton resonances is comparatively small.

The self-association process in aqueous solution is highly dynamic with molecules constantly associating and dissociating.<sup>33</sup> The hypothetical immobilization of monomers in a sort of one-dimensional crystals, would lead to the line broadening and finally to disappearance of the corresponding NMR resonances. Accordingly the lack of a significant line broadening in the measured spectra is a powerful argument to consider the aggregates as extremely dynamic objects, the monomers, entering or leaving the structure very frequently.

The relevant effects are clearly evidenced in Figure 10, where the relative displacement of the chemical shifts obtained by  $^1\text{H}$  NMR measurements can be compared with those predicted by the DK model in the entire range of investigated ciprofloxacin concentrations. The fact that the three aromatic protons are most affected by the self-association reveals the key role of the 4-quinolone ring in the aggregates growth. As the  $\pi$ – $\pi$  stacking is a short-range interaction, one can assert that the experimental results confirm the isoenthalpic hypothesis used as a fundamental assumption for deriving the predictions of the DK-model.

Starting from the measured data the fitting procedure presented above has been applied to obtain the unknown



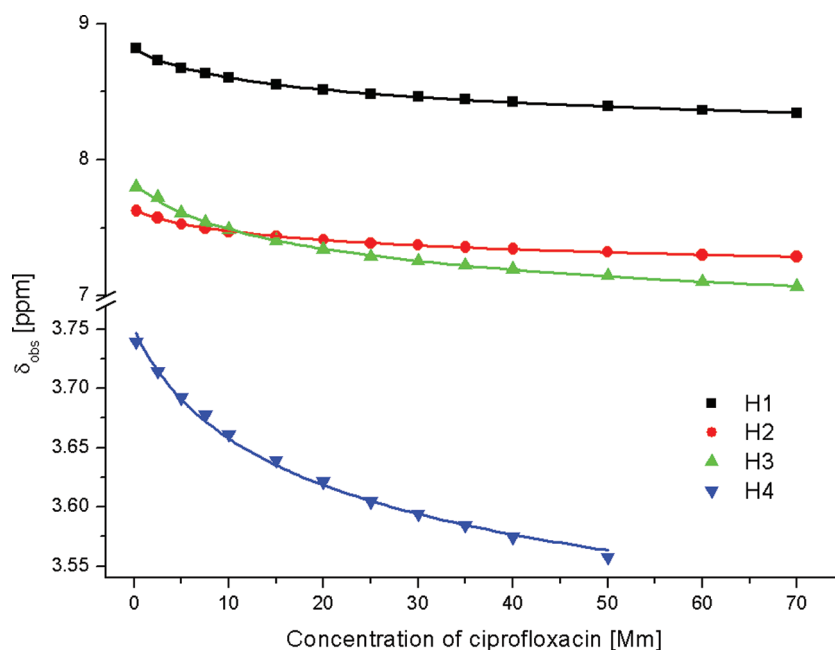


**Figure 9.** Concentration dependences of chemical shifts of several protons of ciprofloxacin in aqueous solution. The fitting curves corresponding to each data set have been obtained with the Origin's multiple data best fit facility, adapted for the DK model.

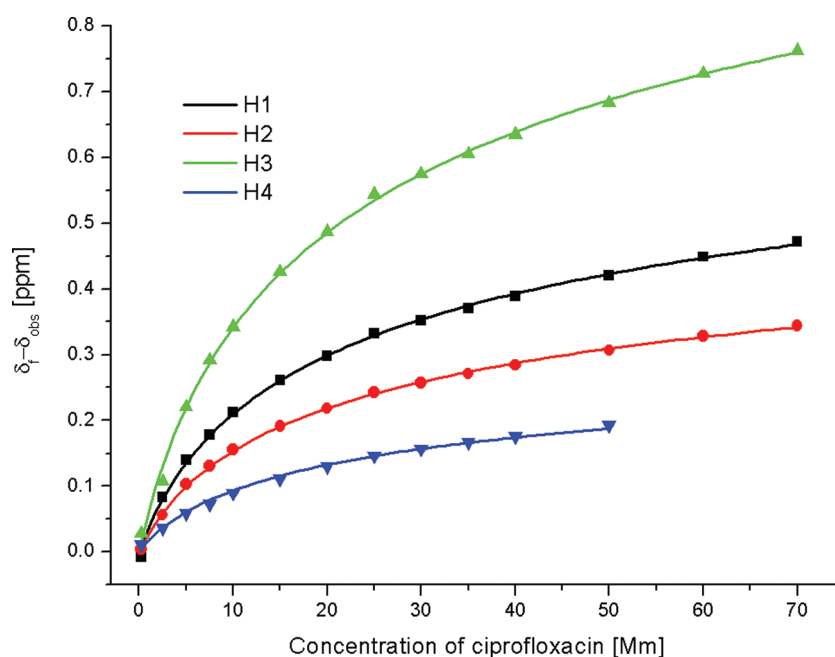


**Figure 10.** Concentration dependences of the relative  $^1\text{H}$  NMR chemical shifts.

**Table 1. Chemical Shifts and Association Constant for Ciprofloxacin Self-Aggregation in Aqueous Solution**

	H1	H2	H3	H4
$\delta_i$ [ppm]	$8.814 \pm 0.004$	$7.629 \pm 0.004$	$7.831 \pm 0.005$	$3.751 \pm 0.004$
$\delta_o$ [ppm]	$7.543 \pm 0.075$	$6.700 \pm 0.057$	$5.765 \pm 0.120$	$3.187 \pm 0.037$
$\Delta\delta$ [ppm]	$1.271 \pm 0.071$	$0.929 \pm 0.053$	$2.066 \pm 0.115$	$0.564 \pm 0.033$
$K_0$ [ $\text{M}^{-1}$ ]		$7.097 \pm 0.770$		
$\Gamma$ [ $\text{M}^{-1}$ ]		$0.360 \pm 0.173$		

parameters  $K$ ,  $\delta_o$ , and  $\delta_i$  returned by the DK model. The mean values of the calculated parameters are presented in Table 1.

The obtained values reveal two main aspects: (i) the association constant is small due probably to the fact that the

$\pi$ - $\pi$  attractive interaction is weakened by the repulsive electrostatic component and (ii) the nonideality is also small ( $\Gamma X_t < 0.025$  in the entire domain of concentrations) so that the DK model is suitable to describe the investigated molecular

system. In order to have a comparative view of the results obtained by fitting the  $^1\text{H}$  NMR measured data with different self-association models we list the corresponding dimerization constants  $K_2$ :  $65.87 \pm 5.29 \text{ M}^{-1}$  (EK),  $53.51 \pm 4.45 \text{ M}^{-1}$  (AK),  $28.39 \pm 3.08 \text{ M}^{-1}$  (DK), and  $32.93 \pm 2.64 \text{ M}^{-1}$  (D). The obtained values are, all of them, relatively small and consequently self-association becomes relevant only for concentrations higher than 1 mM.

In the final part of this section we will emphasize several intriguing aspects that must be overcome in the difficult task of choosing the most suitable model. In this respect one must not forget that even if the isodesmic stacking and the simple dimerization process predict completely different aggregates size distributions, the variation of the NMR chemical shifts become formally indistinguishable<sup>40</sup> if the reasonable hypothesis related to the additivity of the upfield shift brought by the neighbors is used. The two simple models mentioned above provide both of them analytic formula that become identical if the equilibrium self-association constant for the EK-model is two times larger than those corresponding to the D-model.<sup>40</sup> It is only one illustration of the fact that fitting accuracy is not a decisive argument for the correctness of the selected model. The relatively smooth variations obtained in a NMR experiment can be fitted with comparable precisions using all of the mentioned models. The main argument that we bring to support the DK model is not related to the accuracy of the data fit but to the well-fundamented statistical thermodynamical approach.

## CONCLUSION

The  $\pi$ - $\pi$  stacking is an important noncovalent interaction between aromatic molecules having a ubiquitous presence and being the main source of the short-range intermolecular attractive force. Even if the self-association (dissociation) processes can be taken as iso-enthalpic in the first approximation, the entropic effects impose a particular dependence of the equilibrium constants on the size of the associating aggregates. Starting with very general statistical thermodynamical hypothesis, we have found the explicit expression of the association constant  $K_{n,m}$  which govern the equilibrium for an association-dissociation process between two aggregates with  $n$  and  $m$  monomers respectively. For the particular case of stepwise self-association processes  $X_{n-1} + X \xrightleftharpoons{K_n \equiv K_{n-1,1}} X_n$  there are several models which predict quite different relation between  $K_n$  and  $n$ . Our predictions confirm the results published several years ago.<sup>19</sup> We have found also the explicit expressions which describe the equilibrium size distribution of aggregates which has been used after that to find the mean number of monomers in an aggregate. All information mentioned above can be obtained if one known only two parameters: the total concentration of monomers and the dimerization constant  $K_2$ . The model can be also extended for the nonideal molecular systems if the nonassociative interactions between aggregates are weak as compared to the associative ones. The developed theoretical approach was tested on the NMR data obtained from ciprofloxacin self-association experiments. Our theoretical predictions are able to fit very accurately the measured data, but we consider that more important than the accuracy of the data fit is the robustness of the proposed model and the well-fundamented approach. The theoretical approach does not use any empirical conjectures relying only on firm statistical thermodynamical arguments.

## AUTHOR INFORMATION

### Corresponding Author

\*E-mail: ioan.turcu@itim-cj.ro; mircea.bogdan@itim-cj.ro.

### Notes

The authors declare no competing financial interest.

## ACKNOWLEDGMENTS

This work was financially supported by UEFISCDI Romania, Projects PCE No. 8/2011 and PCCE-ID 76.

## REFERENCES

- (1) Zang, L.; Che, Y.; Moore, J. S. *Acc. Chem. Res.* **2008**, *41*, 1596–1608.
- (2) Davis, J. T. *Angew. Chem., Int. Ed.* **2004**, *43*, 668–698.
- (3) Zhao, Y. S.; Fu, H.; Peng, A.; Ma, Y.; Liao, Q.; Yao, J. *Acc. Chem. Res.* **2010**, *43*, 409–418.
- (4) Zhang, S. *Biotechnol. Adv.* **2002**, *20*, 321–339.
- (5) Kwon, S.; Shin, H. S.; Gong, J.; Eom, J.-H.; Jeon, A.; Yoo, S. H.; Chung, I. Si.; Cho, S. J.; Lee, H.-S. *J. Am. Chem. Soc.* **2011**, *133*, 17618–17621.
- (6) Rzepecki, P.; Hochdörffer, K.; Schaller, T.; Zienau, J.; Harms, K.; Ochsenfeld, C.; Xie, X.; Schrader, T. *J. Am. Chem. Soc.* **2008**, *130*, 586–591.
- (7) Davies, D. B.; Djimant, L. N.; Veselkov, A. N. *J. Chem. Soc., Faraday Trans.* **1996**, *92*, 383–390.
- (8) Sigel, H.; Griesser, R. *Chem. Soc. Rev.* **2005**, *34*, 875–900.
- (9) Wong, A.; Ida, R.; Spindler, L.; Wu, G. J. *Am. Chem. Soc.* **2005**, *127*, 6990–6998.
- (10) Sanna, C.; La Mesa, C.; Mannina, L.; Stano, P.; Viel, S.; Segre, A. *Langmuir* **2006**, *22*, 6031–6041.
- (11) Evstigneev, M. P.; Evstigneev, V. P.; Davies, D. B. *J. Chem. Phys.* **2007**, *127*, 154511.
- (12) Duffy, E. M.; Jorgensen, W. L. *J. Am. Chem. Soc.* **2000**, *122*, 2878–2888.
- (13) Wang, J.; Wang, W.; Huo, S.; Lee, M.; Kollman, P. A. *J. Phys. Chem. B* **2001**, *105*, 5055–5067.
- (14) Garland, F.; Christian, S. D. *J. Phys. Chem.* **1975**, *79*, 1247–1252.
- (15) Hill, T. L. *Biophys. J.* **1983**, *44*, 285–288.
- (16) Chatelier, R. C. *Biophys. Chem.* **1987**, *28*, 121–128.
- (17) Attwood, D. *Adv. Colloid Interface Sci.* **1995**, *55*, 271–303.
- (18) Martin, R. B. *Chem. Rev.* **1996**, *96*, 3043–3064.
- (19) (a) Beshnova, D. A.; Lantushenko, A. O.; Davies, D. B.; Evstigneev, M. P. *J. Chem. Phys.* **2009**, *130*, 165105–7. (b) Beshnova, D. A.; Lantushenko, A. O.; Evstigneev, M. P. *Ukr. J. Phys.* **2009**, *54*, 355–340.
- (20) Hill, T. L.; Chen, Y.-D. *Biopolymers* **1973**, *12*, 1285–1312.
- (21) Bastian, M.; Sigel, H. *Biophys. Chem.* **1997**, *67*, 27–34.
- (22) Robinson, B. H.; Löffler, A.; Schwar, G. *J. Chem. Soc., Faraday Trans. 1* **1973**, *69*, 56–69.
- (23) Ben-Naim, A. *Curr. Opin. Struct. Biol.* **1994**, *4*, 264–268.
- (24) Bende, A.; Grosu, I.; Turcu, I. *J. Phys. Chem. A* **2010**, *114*, 12479–12489.
- (25) Bende, A.; Turcu, I. *Int. J. Mol. Sci.* **2011**, *12*, 3102–3116.
- (26) Manning, G. S. *J. Phys. Chem. B* **2007**, *111*, 8554–8559.
- (27) Scott, D. J.; Winzor, D. J. *Biophys. J.* **2009**, *97*, 886–896.
- (28) Wills, P. R.; Winzor, D. J. *Biophys. Chem.* **2011**, *158*, 21–25.
- (29) Minami H.; Iwahashi, M. *Int. J. Spectrosc.* **2011**, Article ID 640121.
- (30) Poon, G. M. K. *Anal. Biochem.* **2010**, *400*, 229–236.
- (31) Cal, K.; Centkowska, K. *Eur. J. Pharm. Biopharm.* **2008**, *68*, 467–478.
- (32) Bogdan, M.; Caira, M.; Farcas, S. I. *Supramol. Chem.* **2002**, *14*, 427–436.
- (33) Maurer, N.; Wong, K. F.; Hope, M. J.; Cullis, P. R. *Biochim. Biophys. Acta* **1998**, *1374*, 9–20.
- (34) Abbott, L. C.; Batchelor, S. N.; Oakes, J.; Lindsay Smith, J. R.; Moore, J. N. *J. Phys. Chem. B* **2004**, *108*, 13726–13735.
- (35) Lyles, M. B.; Cameron, I. L. *Biophys. Chem.* **2002**, *96*, 53–76.

- (36) Sun, H.; Ye, K.; Wang, C.; Qi, H.; Li, F.; Wang, Y. *J. Phys. Chem. A* **2006**, *110*, 10750–10756.
- (37) Kostjukov, V. V.; Pahomov, V. I.; Andrejuk, D. D.; Davies, D. B.; Evstigneev, M. P. *J. Mol. Struct.* **2007**, *843*, 78–86.
- (38) Michaleas, S.; Antoniadou – Vyza, E. *J. Pharm. Biomed. Anal.* **2006**, *42*, 405–410.
- (39) Riley, C. M.; Ross, D. L.; van der Velder, D.; Takusagawa, F. *J. Pharm. Biomed. Anal.* **1993**, *11*, 49–59.
- (40) Mitchell, P. R.; Sigel, H. *Eur. J. Biochem.* **1978**, *88*, 149–154.